Electronic Materials Letters, Vol. 4, No. 4 (2008), pp. 161-165

Large Scale Fabrication of Single-Crystal CuO Nanoplatelets Using a Template-Free Hydrothermal Approach

Huiyu Chen,[1] Sung-Min Park,[2] Jong-Hak Lee,[2] Xianhui Meng,[1] Dong-Wook Shin,[2] and Ji-Beom Yoo[1,2,*]

[1]School of Advanced Materials Science & Engineering (BK21), Sungkyunkwan University, Suwon 440-746, Korea
[2]SKKU Advanced Institute of Nanotechnology (SAINT), Sungkyunkwan University, Suwon 440-476, Korea

This paper reports the large scale production of CuO nanoplatelets with smooth surface using a simple hydrothermal method in a water and ethanol solution without any templates or additives. The micro-structure and morphology of the CuO nanoplatelets were examined by X-ray diffraction, Raman spectra, field emission scanning electron microscopy and transmission electron microscopy. The CuO nanoplatelets were monoclinic, and their length and width ranged from 100 to 300 nm and 80 to 120 nm, respectively. A possible growth mechanism for the formation of CuO nanoplatelets was proposed. The volume ratio of ethanol in the solution was found to be a critical effect on the CuO morphology during the hydrothermal stage. The band gap of the CuO nanoplatelets was estimated to be 2.13 eV from the UV-vis spectra.

Keywords: CuO nanoplatelets, hydrothermal method, template-free

1. INTRODUCTION

Over the past few decades, the fabrication of inorganic nanostructures with a well-controlled morphology has attracted considerable attention because the physical and chemical properties of these materials are closely related to their shape, crystalline structure and size.[1,2] Studies on one-dimensional (1D) and two-dimensional (2D) nanostructures, such as nanowires, nanotubes, nanobelts, nanoribbons and nanoplatelets, have been expanding rapidly due to the wide range of potential applications in nanodevices.[3-5] Generally, hard templates (AAO, CNTs, porous membranes) and soft templates (capping reagents, surfactants) are employed for the morphology controlled synthesis of these nanostructure.[3,6] However, the template method is difficult to handle, and complicated post-synthesis treatment is required in order to harvest the resultant products. Therefore, it is promising to develop a template-free route for the synthesis of nano- or micro-scale materials.

CuO is an important p-type semiconductor with a narrow band gap (E_g = 1.2 eV) and has many practical applications in sensors, catalysts and solar cells.[7-9] It also forms the basis of several high-T_c superconductors and materials with giant magnetoresistance.[10] Up to now, many synthetic approaches have been used to prepare nanostructured CuO in order to enhance its performance in currently existing applications.[11-18] Zhang et al. fabricated assembly CuO hollow spheres and nanoshuttles.[19,20] Zeng and co-workers reported the synthesis of dandelion-shaped hollow structures, self-assembly of CuO nanorods and nanoribbons.[21,22]

In this paper, CuO nanoplatelets with smooth surface were synthesized on a large scale without templates or additives. To the best of our knowledge, this is the first report of the preparation of CuO nanoplatelets using a template-free hydrothermal method in a water and ethanol solution system. This work may provide new insights into the fabrication of other 2D nanostructures.

2. EXPERIMENT

In a typical procedure, 9 mmol $CuCl_2 \cdot 2H_2O$ (99% purity Sigma-Aldrich) was dissolved in 250 mL of an ethanol and water solution (v/v = 2:1). 20 mL NaOH (5 M, in distilled water) was then added with constant stirring. The final mixture was transferred to a 375 mL Teflon-lined stainless steel autoclave and maintained at 150°C for 16 h in an electric oven. After the reaction, the autoclave was allowed to cool naturally to room temperature. The precipitate was collected, rinsed several times with distilled water and absolute ethanol and finally dried at 40°C in air for 10 h.

The x-ray diffraction (XRD) pattern was collected using a Bruker D8 focus diffractometer with Cu Kα radiation (λ = 1.5406 Å) in the 2θ range of 30° to 80° at a scan rate of

*Corresponding author: jbyoo@skku.edu

4°/min. The Raman spectra were obtained from 200 to 700 cm^{-1} at room temperature using an excitation energy of 514 nm at 20 mW (RM1000-Invia, Renishaw). The SEM images were obtained using a field emission scanning electron microscope (FESEM, JEOL JSM6700F). The transmission electron microscopy (TEM and HRTEM) images as well as the corresponding selected area electron diffraction (SAED) patterns were obtained using a JEOL JEM2100F instrument at an accelerating voltage of 200 kV. The UV-vis absorption spectrum of the as-prepared products was recorded using a UV-vis-NIR spectrophotometer (SHIMADZU, UV-3600)

3. RESULTS AND DISCUSSION

Figure 1 shows the XRD pattern of the as-prepared CuO sample. All the peaks were indexed to a monoclinic phase CuO (JCPDS File No.5-0661). No impurities such as $Cu(OH)_2$ or Cu_2O, were detected, indicating that the CuO products obtained through the current synthetic approach were a pure phase.

CuO has a monoclinic structure and belongs to the c_{2h}^6 space group, which contains two molecular units per unit cell. Therefore, there are 12 zone-center vibrational modes including three acoustic modes ($A_u + 2B_u$), six infrared active modes ($3A_u + 3B_u$) and three Raman active modes ($A_g + 2B_g$). Figure 2 shows the room temperature Raman spectrum of the as-obtained CuO sample. The three Raman peaks at 611, 317 and 277 cm^{-1} were assigned to B_g, B_g and A_g modes, respectively, through a comparison with the vibrational spectra of a CuO single crystal.[23] The results are in agreement with the value reported in the literature, which indicates that the as-synthesized product consists of single phase CuO with a monoclinic structure.

The morphology and microstructure of the obtained CuO product were examined by FESEM and TEM. Platelet-like (nanoplatelets) CuO structures with smooth surface were detected from the FESEM image in Fig. 3a. The length and width of the nanoplatelets are up to 100-300 nm and 80-120 nm, respectively. A closer observation indicated that the shapes of the nanoplatelets were not perfect rectangles but showed small zigzags in the edges. Figure 3b shows a typical TEM image, from which the size of the CuO nanoplatelets is in accordance with that observed in the FESEM image. The SAED pattern of the single nanoplatelet shown in the inset of Figure 3b was indexed to the [001] zone axis, indicating the single crystalline CuO nanoplatelets with a monoclinic structure. The pattern spots were consistent with the XRD results. Figure 3c shows a HRTEM image of a nanoplatelet with a lattice fringe at a constant spacing of 0.269 nm, which corresponds to that of the $(\bar{1}10)$ planes of CuO. HRTEM and SAED analysis showed that the nanoplatelets grew along the [010] direction.

During the reaction process, the ethanol to water volume ratio in the mixed solution system played an important role in controlling the synthesis of CuO nanoplatelets. When no ethanol was added to the system with the other experimental parameters kept the same as those in the typical synthesis, the reaction only produced some layered agglomerates (Fig. 4a) with a larger size. However, when the system contained a small amount of ethanol, the resultant products were composed of nanoplatelets and agglomerates, as shown in Fig. 4(b). When ethanol was the main component in the mixed solution (ethanol/water = 4:1, v/v), the final CuO nanoplatelets existed with irregular shapes and a non-uniform size. In addition, many small nanopatches were also obtained simultaneously (Fig. 4c).

From the above comparative experiments, a possible mechanism for the formation of CuO nanoplatelets was proposed, which is different from the reported route that the surfactant was involved.[18] At the initial stage, the orthorhombic $Cu(OH)_2$ precursor precipitated as small nanoribbons or nan-

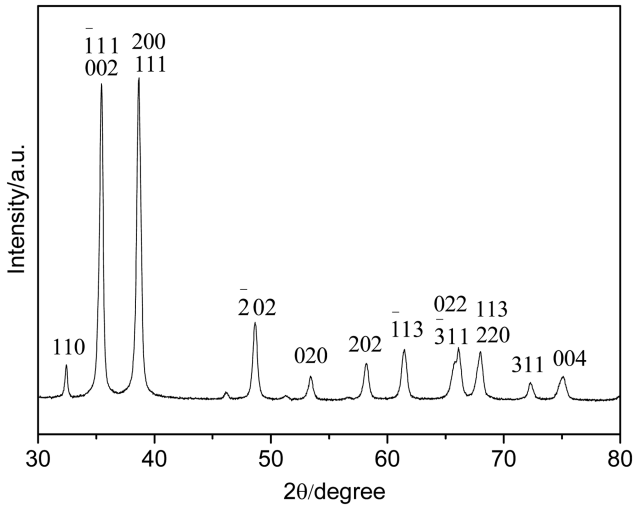

Fig. 1. The XRD pattern of the as-prepared CuO product.

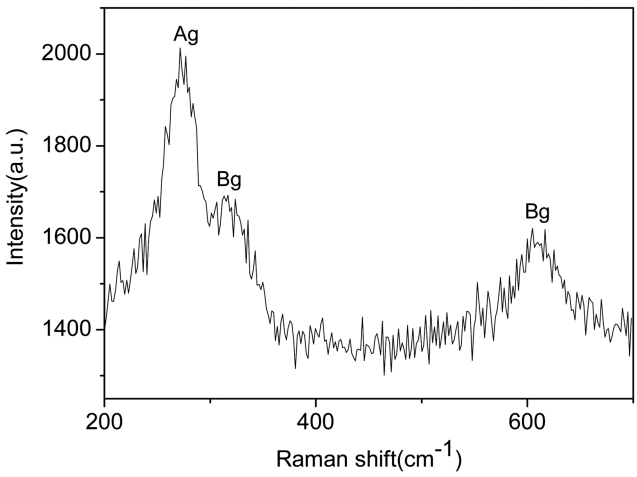

Fig. 2. The Raman spectra of the as-prepared CuO product.

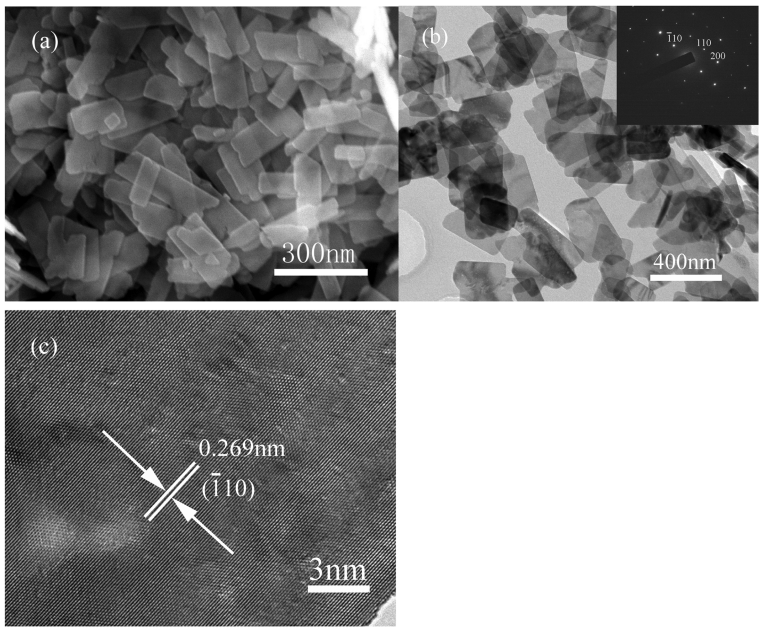

Fig. 3. (a) FESEM image and (b) TEM image of CuO nanoplatelets; The upper inset of (b) shows the corresponding SAED pattern of the individual nanoplatelet obtained by focusing the electron beam along the [001] zone axis; (c) HRTEM image of the nanoplatelet.

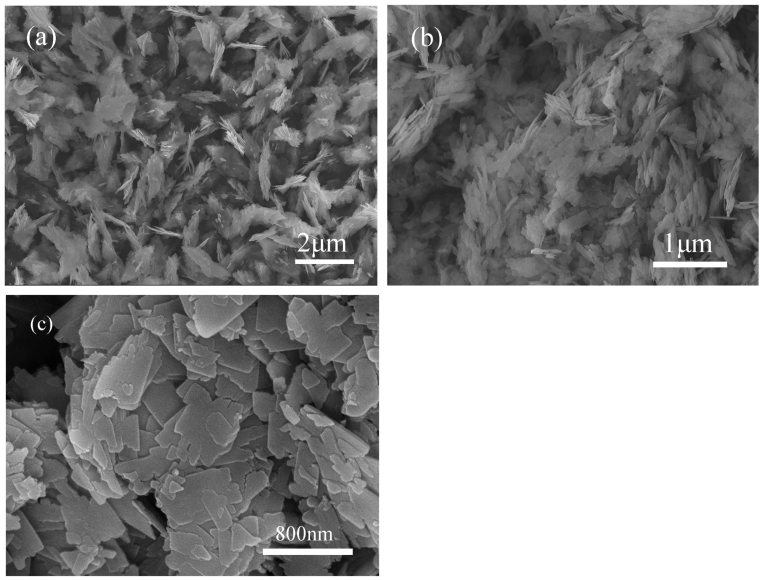

Fig. 4. SEM images of the products obtained in the water system (a); in the ethanol and water mixture (b) v/v = 1:2 and (c) v/v = 4:1.

orods due to the connection of the (010) planes through H-bonds.[25,26] In the following hydrothermal period, $Cu(OH)_2$ lost H_2O molecules by breaking the interplanar H-bonds, resulting in the formation of layered monoclinic CuO nanostructures. Therefore, layered CuO agglomerates or small amounts of nanoplatelets were obtained in the pure water system or in the solution with a low volume ratio of ethanol. Ethanol has a lower surface tension than water, which had a significant effect on the nucleation and dispersion of the $Cu(OH)_2$ precursor. Consequently, $Cu(OH)_2$ was dehydrated more easily in a mixed solution with a higher ethanol concentration, which leads to the final CuO nanostructure with smooth surface. The detailed formation mechanism of the CuO nanoplatelets as well as the effect of the ethanol ratio in the solution mixtures on the CuO morphology requires further investigation.

UV-vis absorption measurements are one of the most effective methods for examining the optical properties of semiconductor nanomaterials. Figure 5a shows the UV-vis absorption spectrum of the as-prepared nanoplatelets dispersed in absolute ethanol. The result shows a broad absorption peak centered at approximately 370 nm. An estimate of

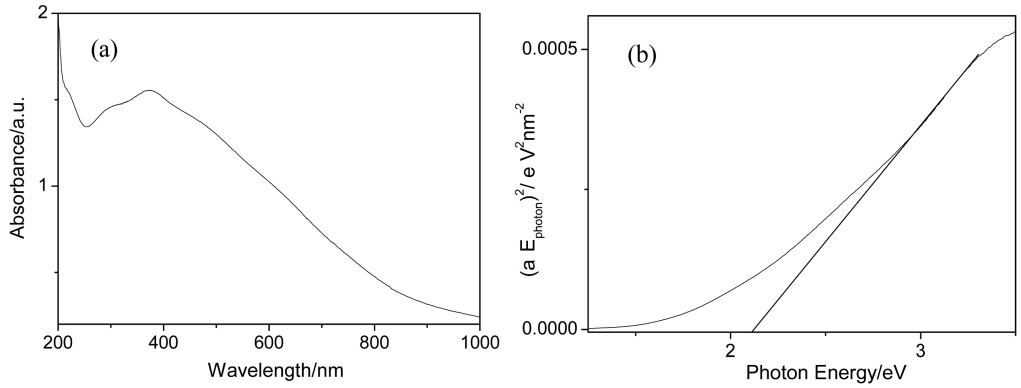

Fig. 5. (a) UV-vis absorption spectrum of the CuO nanoplatelets; (b) The corresponding plots of $(\alpha E_{photon})^2$ vs E_{photon} for the direct transitions.

the optical band gap was obtained using the equation $\alpha E_{photon} = K(E_{photon} - E_g)^{1/2}$ (where α is the absorption coefficient, K is a constant and E_g is the band gap energy).[24] Figure 5b shows a plot of $(\alpha E_{photon})^2$ vs E_{photon} for a direct transition. Extrapolation to $\alpha = 0$ (the straight line to the X-axis) gives the absorption edge energy corresponding to an $E_g = 2.13$ eV, which shows a significant blue-shift compared with that of bulk CuO (1.2 eV). Therefore, there are probably some CuO nanoparticles with very small size or a very minute component of $Cu_{1+x}O$ present. The high band gap of 2.13 eV is possibly due to both the minute impurities and nanoplatelets structures.

4. CONCLUSIONS

In summary, CuO nanoplatelets were fabricated successfully using a simple and efficient hydrothermal method. No additives, surfactants or templates were used in the synthetic route. The results indicated that a mixed solution system of water and ethanol plays a key role in the formation of nanoplatelets. These 2D CuO nanostructures are expected to have a variety of applications and the current synthetic approach may provide some insights in the preparation of other 2D inorganic nanomaterials.

ACKNOWLEDGEMENT

The financial support from the BK21 Project of School of Advanced Materials Science & Engineering is gratefully acknowledged.

REFERENCES

1. K. Nagaveni, A. Gayen, G. N. Subbanna, and M. S. Hegde, *J. Mater. Chem.* **12**, 3147 (2002).
2. Y. G. Sun and Y. N. Xia, *Science* **298**, 2176 (2002).
3. Y. N. Xia, P. D. Yang, Y. G. Sun, Y. Y. Wu, B. Mayers, B. Gates, Y. D. Yin, F. Kim, and Y. Q. Yan, *Adv. Mater.* **15**, 353 (2003).
4. Z. W. Pan, Z. R. Dai, and Z. L. Wang, *Science* **291**, 1947 (2001).
5. J. W. Kim, J. S. Hong, and K. S. Lee, *Electron. Mater. Lett.* **3**, 169 (2007).
6. C. Bae, H. Yoo, S. Kim, K. Lee, J. Kim, M. M. Sung, and H. Shin, *Chem. Mater.* **20**, 756 (2008).
7. A. Chowdhuri, V. Gupta, K. Sreenivas, R. Kumar, S. Mozumdar, and P. K. Patanjali, *Appl. Phys. Lett.* **84**, 1180 (2004).
8. A. L. Sauvet and J. Fouletier, *J. Power Sources* **101**, 259 (2001).
9. J. A. Switzer, H. M. Kothari, P. Poizot, S. Nakanishi, and E. W. Bohannan, *Nature* **425**, 490 (2003).
10. H. Takeda and K. Yoshino, *Phys. Rev. B* **67**, 5109 (2003).
11. X. Q. Wang, G. C. Xi, S. L. Xiong, Y. K. Liu, B. J. Xi, W. C. Yu, and Y. T. Qian, *Crystal Growth and Design* **7**, 930 (2007).
12. G. F. Zou, H. Li, D. W. Zhang, K. Xiong, C. Dong, and Y. T. Qian, *J. Phys. Chem. B* **110**, 1632 (2006).
13. H. M. Xiao, S. Y. Fu, L. P. Zhu, Y. Q. Li, and G. Yang, *Eur. J. Inorg. Chem*. 1966 (2007).
14. Q. Liu, Y. Y. Liang, H. J. Liu, J. M. Hong, and Z. Xu, *Mater. Chem. Phys.* **98**, 519 (2006).
15. Y. Y. Xu, D. R. Chen, X. L. Jiao, and K. Y. Xue, *Mater. Res. Bull*. **42**, 1723 (2007).
16. D. Keyson, D. P. Volanti, L. S. Cavalcante, A. Z. Simoes, J. A. Varela, and E. Longo, *Mater. Res. Bull.* **43**, 771 (2008).
17. K. B. Zhou, R. P. Wang, B. Q. Xu, and Y. D. Li, *Nanotechnology* **17**, 3939 (2006).
18. Q. Liu, H. J. Liu, Y. Y. Liang, Z. Xu, and G. Yin, *Mater. Res. Bull*. **41**, 697 (2006).
19. Y. G. Zhang, S. T. Wang, X. Wang, Y. T. Qian, and Z. D. Zhang, *J. Nanosci. Nanotechnol*. **6**, 1423 (2006).
20. Y. G. Zhang, S. T. Wang, X. B. Li, L. Y. Chen, Y. T. Qian, and Z. D. Zhang, *J. Crystal Growth* **291**, 196 (2006).
21. B. Liu and H. C. Zeng, *J. Am. Chem. Soc*. **126**, 8124 (2004).
22. Y. Chang and H. C. Zeng, *Crystal Growth and Design* **4**, 397 (2004).

23. J. C. Irwin, J. Chrzanowski, and T. Wei, *Physica C* **166**, 456 (1990).
24. S. Tsunekawa and T. Fukuda, *J. Appl. Phys*. **87**, 1318 (2000).
25. W. X. Zhang, X. G. Wen, and S. H. Yang, *Inorg. Chem*. **42**, 5005 (2003).
26. Z. H. Yang, J. Xu, W. X. Zhang, A. P. Liu, and S. P. Tang, *J. Solid State Chem*. **180**, 1390 (2007).